

AperTO - Archivio Istituzionale Open Access dell'Università di Torino

**Xanthan-Based Hydrogel for Stable and Efficient Quasi-Solid Truly Aqueous Dye-Sensitized Solar Cell with Cobalt Mediator**

**This is a pre print version of the following article:**

*Original Citation:*

*Availability:*

This version is available <http://hdl.handle.net/2318/1803879> since 2021-09-22T13:15:06Z

*Published version:*

DOI:10.1002/solr.202000823

*Terms of use:*

Open Access

Anyone can freely access the full text of works made available as "Open Access". Works made available under a Creative Commons license can be used according to the terms and conditions of said license. Use of all other works requires consent of the right holder (author or publisher) if not exempted from copyright protection by the applicable law.

(Article begins on next page)

## **Xanthan-based hydrogel for stable and efficient quasi-solid truly aqueous DSSC with cobalt mediator**

*Simone Galliano, Federico Bella\*, Matteo Bonomo\*, Fabrizio Giordano, Michael Grätzel, Guido Viscardi, Anders Hagfeldt, Claudio Gerbaldi, Claudia Barolo*

### **DISCLAIMER**

**THIS DOCUMENT IS THE NOT PAGINATED VERSION OF THE ARTICLE: “Xanthan-based hydrogel for stable and efficient quasi-solid truly aqueous DSSC with cobalt mediator”. PLEASE DOWNLOAD THE FINAL PAGINATED VERSION AT <https://pubs.rsc.org/en/content/articlelanding/2018/cp/c8cp06728g#!divAbstract>**

Dr. S. Galliano, Dr. M. Bonomo, Prof. G. Viscardi, Prof. C. Barolo  
Department of Chemistry, NIS Interdepartmental Centre and INSTM Reference Centre,  
Università degli Studi di Torino, Via Pietro Giuria 7, 10125 – Torino, Italy  
E-mail: [matteo.bonomo@unito.it](mailto:matteo.bonomo@unito.it)

Prof. F. Bella  
Department of Applied Science and Technology, Politecnico di Torino, Corso Duca degli  
Abruzzi 24, 10129 – Torino, Italy  
E-mail: [federico.bella@polito.it](mailto:federico.bella@polito.it)

Dr. F. Giordano, Prof. M. Grätzel, Prof. A. Hagfeldt  
Laboratory of Photonics and Interfaces, Institute of Chemical Sciences and Engineering,  
School of Basic Sciences, Ecole Polytechnique Fédérale de Lausanne, CH-1015 – Lausanne,  
Switzerland

Prof. C. Gerbaldi  
GAME Lab, Department of Applied Science and Technology, Politecnico di Torino, Corso  
Duca degli Abruzzi 24, 10129 – Torino, Italy

Prof. C. Barolo  
ICxT Interdepartmental Centre, Università degli Studi di Torino, Via Lungo Dora Siena 100,  
10153 – Turin, Italy

**Keywords:** (Dye-sensitized solar cell, Cobalt redox couple, Aqueous electrolyte, Design of Experiment, Xanthan gum)

**Abstract text.** Aqueous dye-sensitized solar cells are emerging as a promising alternative to enhance both the lifetime and environmental friendliness of traditional DSSCs. In this article, we report a cobalt-based, jellified (with xanthan gum) aqueous electrolyte, leading to a valuable efficiency exceeding 4% ( $V_{OC} = 847$  mV,  $J_{SC} = 6.73$  mA cm<sup>-2</sup>, FF = 74%). Design of experiment is employed to precisely and significantly study, at a multivariate level, the effects produced by

$\text{Co}^{2+}$  concentration,  $\text{Co}^{2+}/\text{Co}^{3+}$  ratio and xanthan gum amount modifications on the overall photovoltaic parameters of lab-scale solar cells.

## 1. Introduction

Since the discovery of dye sensitized solar cells (DSSCs), the most frequently used redox mediator has been the iodide/triiodide couple ( $\text{I}^-/\text{I}_3^-$ ).<sup>[1]</sup> However, though it leads to efficient sensitizer regeneration and slow recombination kinetic with the electrons in the  $\text{TiO}_2$  conduction band, its redox potential limits the maximum open-circuit voltage ( $V_{\text{OC}}$ ) deliverable by the device and the strong light absorption of  $\text{I}_3^-$  restricts the application in transparent and tandem devices.<sup>[2,3]</sup> Furthermore, the iodine-based couple was proven to be unsuitable for large scale applications, being corrosive toward copper/silver electrodes used to collect electrons in modules.<sup>[4,5]</sup>

Alternative redox couples were proposed, based mainly on copper or cobalt complexes, but also on organic compounds.<sup>[6,7]</sup> Among these alternative chemistries, cobalt-based shuttles attracted a wide attention for several reasons:<sup>[8]</sup> (i) their light absorption is weaker than that of iodine-based systems; (ii) they are not corrosive and not volatile, thus enhancing the long-term stability of the device, and (iii) they possess easily tuneable redox potentials (also being, generally, more positive than that of the  $\text{I}^-/\text{I}_3^-$  couple).<sup>[9–11]</sup> In recent years, cobalt complexes have been successfully employed in organic solvent-based DSSCs, leading to remarkable power conversion efficiency (PCE) values of up to 14.3%.<sup>[12]</sup> Best results were obtained with a  $[\text{Co}(\text{phen})_3]^{3+/2+}$  couple, mixed with 11 different additives dissolved in acetonitrile.<sup>[12]</sup>

In view of the commercialization and large-scale deployment of DSSCs, the redox mediator employed notwithstanding, the widely used organic solvents, being highly volatile, could result in electrolyte evaporation and leakage. In this context, DSSCs based on a gel electrolyte can compete with their liquid counterparts in terms of PCE and, importantly, exhibit better long-term stability.<sup>[13–17]</sup> Quasi-solid electrolytes based on iodine have been quite extensively

reported in literature.<sup>[18]</sup> Conversely, just few examples of cobalt-based counterparts have been presented.<sup>[19–21]</sup> This is mainly due to the relatively slow diffusion coefficients of bulky cobalt complexes (*e.g.*,  $1.39 \times 10^{-6} \text{ cm}^2 \text{ s}^{-1}$  for  $[\text{Co}(\text{bpy})_3]^{3+}$  in acetonitrile), that are reduced further (–30%) once incorporated in a gelled matrix.<sup>[19]</sup> As a noteworthy example, Spiccia and co-workers proposed cobalt-based gel electrolytes with 4 wt% of poly(vinylidene fluoride-*co*-hexafluoropropylene) (PVDF-HFP) incorporated in acetonitrile.<sup>[19]</sup> The resulting devices, sensitized with MK2 dye, showed efficiencies up to 8.7% under full sunlight intensity; their short-circuit current density ( $J_{\text{SC}}$ ) and fill factor (FF) decreased when the polymer content was increased up to 10 wt%. This suggested that an increase in the polymer content reduced the diffusion rate of the redox mediator. As regards the long-term stability, the polymeric devices maintained more than 90% of their initial PCE after 700 h under operative conditions. A similar PVDF-based electrolyte (1.5 wt% in methoxypropionitrile) was proposed by Kloo's group to further boost the long term stability without showing any loss in PCE, even after 1000 h aging under ambient conditions.<sup>[20]</sup> An alternative approach, consisting of the *in situ* photopolymerization of polymer electrolytes incorporating the Co(II)/Co(III)-based mediator, was proposed by some of us,<sup>[21]</sup> starting from a mixture of mono- and bifunctional methacrylates mixed with the  $[\text{Co}(\text{bpy})_3]^{3+/2+}$  mediator, all photocrosslinked between cell electrodes. A remarkable PCE of 6.6%, coupled to an outstanding stability exceeding 1200 h, was achieved.

Notwithstanding the remarkable stability independently reached by different groups, the common use of organic solvents (being toxic and flammable) in jellified electrolytes seriously undermines the safety and the sustainability of the resulting solar cells.<sup>[22–24]</sup> Therefore, researchers started considering water-based DSSCs, *i.e.* devices using up to 100% water as a solvent for redox couple and additives.<sup>[25]</sup> Yet, this paradigm shift still requires a whole rethink of the cell components aiming at effectively working in an aqueous environment; therefore, new photoelectrodes,<sup>[26]</sup> sensitizers<sup>[27]</sup> and counterelectrodes<sup>[28,29]</sup> have been (and continue to

be) proposed to target emerging issues, *e.g.* electrodes wettability, hydrolysis of anchoring groups, solubility of higher amounts of redox shuttles, etc.

Even if the water-based approach requires a relevant rethink of DSSCs components and interfaces, only a few works have been published dealing with the development of quasi-solid state aqueous DSSCs (a-DSSCs).<sup>[14,30]</sup> Among them, the only example of device incorporating a cobalt-based redox couple dates back to 2015 by Spiccia and co-workers.<sup>[31]</sup> They combined MK2-sensitized TiO<sub>2</sub> electrodes with a collagen-derived gelatin containing the conventional [Co(bpy)<sub>3</sub>]<sup>2+/3+</sup> mediator. The best performing photoanode led to a PCE of 4.1% under 1 sun illumination ( $J_{SC} = 7.9 \text{ mA cm}^{-2}$ ), yet showing a diffusion-limited behaviour. Their work was focused on a novel nanostructured TiO<sub>2</sub> electrode, while the aspects related to the intrinsic hydrogel electrolyte composition were not thoroughly investigated.

In this communication, we present a new cobalt-based quasi-solid electrolyte for a-DSSCs approaching 5% efficiency. The jellifying agent is xanthan gum (XG),<sup>[32]</sup> a polymeric matrix that we successfully demonstrated in aqueous environment for systems based on the iodine-based redox shuttle.<sup>[33]</sup> Here we also propose design of experiment (DoE) as a powerful tool to simultaneously evaluate the effect of different factors on the overall photovoltaic performance, by reducing the number of experiments and offering a wide overview to the readers on the mutual interactions between the measured variable and experimental conditions.<sup>[34]</sup>

## 2. Discussion

### 2.1. Initial screening

To fabricate our lab-scale a-DSSCs, we started from the Co(bpy)<sup>2+/3+</sup> redox couple (0.13 M Co(bpy)<sub>3</sub>Cl<sub>2</sub> and 0.04 M Co(bpy)<sub>3</sub>Cl<sub>3</sub>) dissolved with 0.4 M N-methylbenzimidazole (NMBI) into a chenodeoxycholic acid (CDCA)-saturated water solution; liquid-state cells led to PCE values of 3.72% ( $J_{SC} = 7.98 \text{ mA cm}^{-2}$ ,  $V_{OC} = 623 \text{ mV}$  and  $FF = 74.8$ ). When the Co(bpy)<sup>2+/3+</sup> redox shuttle was replaced with the Co(bpy-pz)<sup>2+/3+</sup> one, the gain in  $V_{OC}$  was evident (+220 mV), even though it was partially counterbalanced by a slight decrease in  $J_{SC}$ , probably due to

a less effective dye regeneration. Overall, this allowed us to overcome the 4% efficiency threshold ( $\text{PCE} = 4.21\%$ ,  $J_{\text{SC}} = 6.73 \text{ mA cm}^{-2}$ ,  $V_{\text{OC}} = 847 \text{ mV}$  and  $\text{FF} = 73.9$ ), a noteworthy achievement in the field of a-DSSCs. Further investigation on this will be tackled in a forthcoming paper dealing with the systematic study of the electrode/electrolyte interface.

It is also worth mentioning that the best device showed an increase in performance by lowering the source irradiance, achieving a 5.25% PCE under 0.1 sun (**Figure S1**), thus highlighting its suitability for indoor and portable applications. Conversely, the PCE drop at higher irradiance level was mainly due to a non-linear increase of  $J_{\text{SC}}$  with the light intensity. An increased electron recombination with high photogenerated current was also expected and could justify the current limitation, even when no mass transport issue occurred.

## 2.2. Design of Experiment (DoE) on the gelation of the electrolyte

Once promising results were obtained with MK2-sensitized cobalt-based liquid-state a-DSSCs, we decided to plan a DoE to precisely investigate the gelation of these aqueous electrolytes by using the bio-derived and cheap XG polymer.<sup>[32]</sup> Additionally, the gelation of the electrolyte was expected to improve the stability of lab-scale cells with respect to those assembled with the liquid solution containing the  $\text{Co}(\text{bpy-pz})^{2+/3+}$  mediator. It is worth mentioning that the gelation of the electrolyte could also lead to serious drawbacks, such as excessively high viscosity values and, thus, a low diffusion coefficient to guarantee efficient solar cells (especially in the presence of bulky redox couples as in this case).<sup>[6,35]</sup> In our study, the effect of electrolyte gelation was evaluated by changing the amount of XG in the solution from 0 (liquid state) to 3 wt% (gelled state), this being centred around the point of the experimental domain (*i.e.*, 1.5 wt%) corresponding to the minimum threshold to obtain a free-standing hydrogel. Moreover, the XG amount was studied in conjunction with the modification of the  $\text{Co}^{2+}$  complex concentration and its relative ratio with its oxidized counterpart (see **Table 1**). Thanks to the multivariate approach we adopted, this work represents a significant advance

with respect to typical studies where a single factor at a time is varied. Other parameters (dye = MK2, electrolyte solvent = CDCA-saturated water, counter-electrode = Pt) remained unchanged in our experiments. It should be noted that variation of these parameters could also be crucial in the optimization of Co-based aqueous electrolytes and they will be analysed in some forthcoming papers.

**Table 1.** Selected factors and related experimental domains for the DoE-aided investigation.

| Factor                             | Range |      |      |
|------------------------------------|-------|------|------|
|                                    | -1    | 0    | +1   |
| Co <sup>2+</sup> [M]               | 0.14  | 0.21 | 0.28 |
| Co <sup>2+</sup> /Co <sup>3+</sup> | 2     | 3    | 4    |
| XG [wt%]                           | 0     | 1.5  | 3.0  |

A simple but meaningful screening with a 2<sup>3</sup> full factorial design was planned on these three factors according to their variation ranges; the experimental outputs (*i.e.*, the photovoltaic parameters) were assessed under 1 sun irradiation. Following the DoE software (MODDE, version 11.0.2.2309, Umetrics)<sup>[36]</sup> protocol, we carried out two replicates for some cells in order to distinguish – in the subsequent fitting phase – the experimental error from the model error. The complete list of cells and their preparation conditions ([Co<sup>2+</sup> complex], Co<sup>2+</sup>/Co<sup>3+</sup> ratio and XG amount) is shown in **Table 2**, along with the corresponding measured photovoltaic parameters. As previously observed with iodine-based electrolytes,<sup>[33]</sup> a-DSSCs devices exhibited an activation period after device sealing. In our study, cobalt-based cells stabilized their efficiency just after 24 h from sealing, thus photovoltaic parameters were evaluated after this time lapse in our laboratory. Overall, we noticed that measured PCE took rather different values in the studied experimental domain, *i.e.* from 3.21% (cell 11) to 4.47% (cell 17); this means that the selected factors were significant for this study.

To better understand the relationship between analysed factors (inputs) and photovoltaic responses (outputs), a multivariate analysis of the experimental data was computed. The

chemometric model was fitted by means of partial least squares regression.<sup>[36]</sup> Overall, DoE fitting did not show any data outliers, and the coefficient analysis was very useful to highlight some trends and interactions between factors and relative effects on a-DSSCs performance. A more complex DoE, also involving a higher number of factors and experiments, will be presented in a forthcoming paper.

**Table 2.** Photovoltaic parameters of a-DSSCs fabricated following the DoE approach; data shown below were collected ~24 h after device sealing.

| Cell | Co <sup>2+</sup><br>[M] | Co <sup>2+</sup> /Co <sup>3+</sup> | XG<br>[wt%] | V <sub>OC</sub><br>[mV] | J <sub>SC</sub><br>[mA cm <sup>-2</sup> ] | FF<br>[%] | PCE<br>[%] |
|------|-------------------------|------------------------------------|-------------|-------------------------|---|-----------|------------|
| 1    | 0.14                    | 2                                  | 0           | 826                     | 5.55                                      | 80.7      | 3.70       |
| 2    |                         |                                    |             | 813                     | 6.25                                      | 77.0      | 3.94       |
| 3    |                         |                                    |             | 789                     | 5.78                                      | 77.4      | 3.53       |
| 4    | 0.28                    | 2                                  | 0           | 816                     | 5.83                                      | 82.0      | 3.90       |
| 5    |                         |                                    |             | 835                     | 6.60                                      | 75.0      | 4.15       |
| 6    |                         |                                    |             | 830                     | 6.51                                      | 76.0      | 4.10       |
| 7    | 0.28                    | 4                                  | 0           | 774                     | 6.03                                      | 79.7      | 3.72       |
| 8    |                         |                                    |             | 787                     | 6.44                                      | 80.5      | 4.08       |
| 9    |                         |                                    |             | 804                     | 5.47                                      | 75.7      | 3.33       |
| 10   | 0.28                    | 2                                  | 3           | 782                     | 5.38                                      | 78.4      | 3.30       |
| 11   |                         |                                    |             | 785                     | 5.05                                      | 81.0      | 3.21       |
| 12   |                         |                                    |             | 808                     | 7.01                                      | 63.4      | 3.59       |
| 13   | 0.14                    | 4                                  | 3           | 785                     | 6.22                                      | 66.0      | 3.22       |
| 14   |                         |                                    |             | 771                     | 6.39                                      | 71.5      | 3.52       |
| 15   |                         |                                    |             | 769                     | 6.60                                      | 72.9      | 3.70       |
| 16   | 0.28                    | 4                                  | 3           | 785                     | 7.02                                      | 71.9      | 3.96       |
| 17   |                         |                                    |             | 791                     | 7.52                                      | 75.1      | 4.47       |
| 18   |                         |                                    |             | 796                     | 6.29                                      | 75.7      | 3.79       |

The effects of each factor and their interactions, which represent the six coefficients of the chemometric model, can be observed on the resulting photovoltaic responses, as plotted in **Figure S2**. Above all, the most significant coefficients were represented by Co<sup>2+</sup> concentration (green bars) on V<sub>OC</sub> and FF, Co<sup>2+</sup>/Co<sup>3+</sup> ratio (blue bars) on J<sub>SC</sub> and FF, while the amount of XG (yellow bars) affected all the parameters, as largely expected. The simultaneous combination of these effects on the photovoltaic performance can be more easily observed by means of the iso-response plots (**Figure 1**). The main effect occurring when the electrolyte status was



changed from liquid to quasi-solid was a slight lowering of  $V_{OC}$  values of roughly 25 mV (XG = 3 wt%). Similarly, the increase in  $\text{Co}(\text{bpy-pz})^{2+}$  concentration led to lower  $V_{OC}$  values, being the redox potential negatively shifted accordingly to Nernst's equation (**Figure 1A**).

Concerning  $J_{SC}$  values (**Figure 1B**), the presence of the XG matrix slightly decreased the measured photocurrent, especially in the presence of higher concentrations of  $\text{Co}^{2+}$  species. This experimental result was initially attributed to a reduced mobility of electrolyte species (both in the interelectrode space and within  $\text{TiO}_2$  pores), mainly caused by the gelation effect. However, this conclusion appeared to be in opposition to the effects observed on the  $J_{SC}$  values by increasing the  $\text{Co}^{2+}/\text{Co}^{3+}$  ratio; indeed, liquid electrolytes-based cells exhibited higher  $J_{SC}$  values when lowering the concentration of the redox mediators, while the opposite trend was found for quasi-solid state systems. Straightforwardly, the main reason of the lower  $J_{SC}$  observed could be ascribed to a sizeable charge recombination, that particularly occurs in concentrated liquid electrolytes. A further, but tentative, explanation on the lower  $J_{SC}$  detected for quasi-solid a-DSSCs could lie in the possibly unfavourable interaction between XG and NMBI. Indeed, when a liquid electrolyte is used, NMBI tends to lie at the  $\text{TiO}_2$ /electrolyte interface, hampering the recombination and thus increasing voltage. On the other hand, considering quasi-solid electrolytes, XG could partially remove NMBI from the  $\text{TiO}_2$  surface and, in case of concentrated electrolytes, can cause the  $J_{SC}$  drop down due to more probable recombination losses. The presence of NMBI and its interaction with XG, as well as the effect of carboxylic moiety on diffusion kinetic of both  $\text{Co}^{3+}$  and  $\text{Co}^{2+}$  species, will be discussed in a forthcoming paper. It is worth mentioning that the highest  $J_{SC}$ , achieved by one of the samples with XG 1.5 wt% (namely cell 17), which exceeded  $7.5 \text{ mA cm}^{-2}$ , outperformed the liquid counterparts, confirming the non-trivial effect of XG addition on photovoltaic performances.

This also proved that it is possible to obtain a gelled electrolyte (with the minimum amount of XG) that mimics the performance of the liquid electrolyte, being, in turns, much more stable.

FF is slightly negatively affected by both the gelation and the dilution of electrolyte (**Figure 1C**) and this could be related to the raising importance of mass transport limitations.

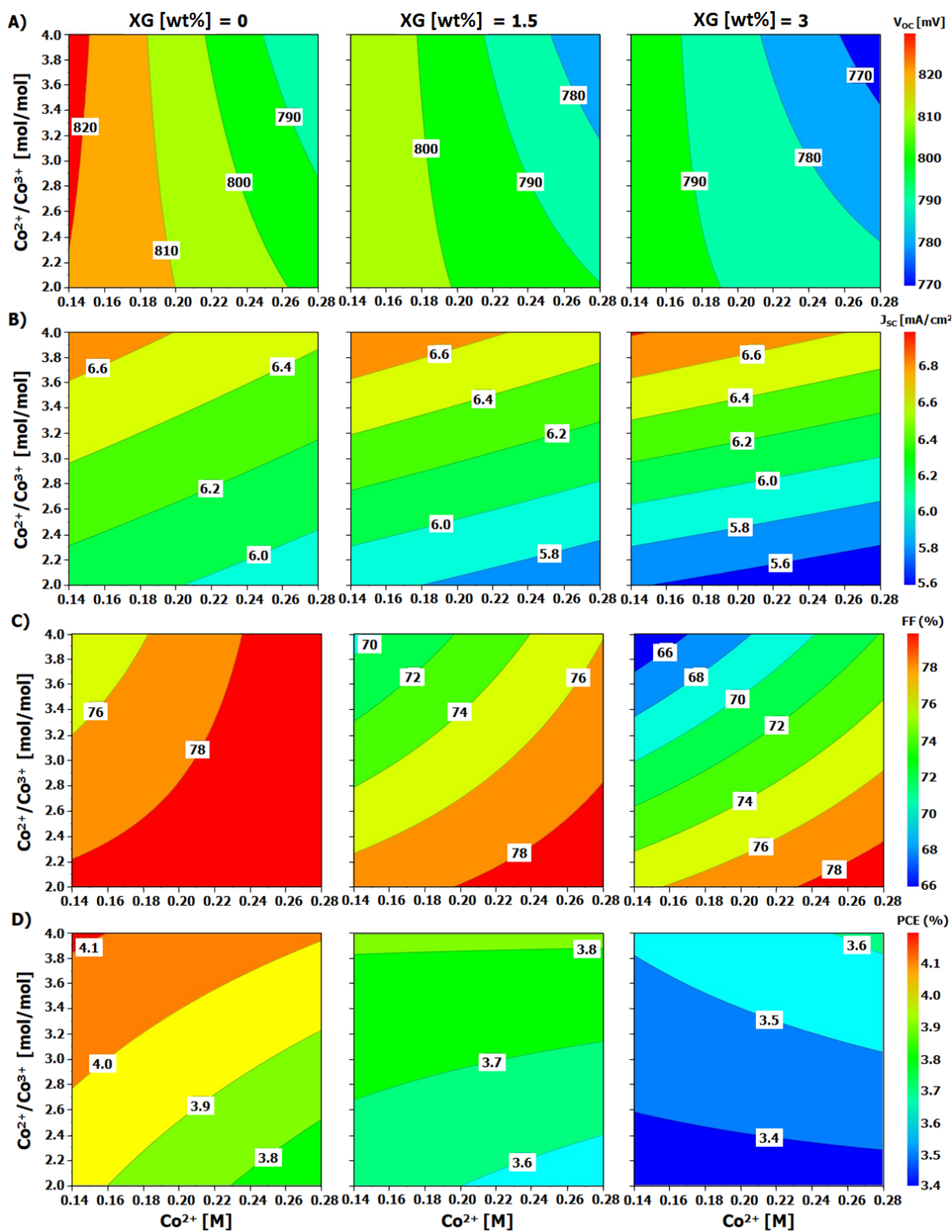


**Figure 1.** Contour plots for V<sub>OC</sub> (A), J<sub>SC</sub> (B), FF (C) and PCE (D) as a function of the explored experimental factors, obtained by fitting the multivariate model.

Finally, the sum of the previous effects due to electrolyte gelation and the change in redox mediator concentrations can be observed on the plot regarding PCE (**Figure 1D**). Generally speaking, the addition of XG tended to slightly decrease the overall PCE, but it was expected to assure a longer stability of the device. Device efficiency values also increased with the  $\text{Co}^{2+}/\text{Co}^{3+}$  ratio, regardless of the physical status of the electrolyte, suggesting the importance of this parameter. Overall, the highest performance was achieved with 1.5 wt% XG, 0.21 M  $\text{Co}^{2+}$  and  $\text{Co}^{2+}/\text{Co}^{3+}$  ratio equal to 3 (*i.e.*, 0.07 M  $\text{Co}^{3+}$ ), which led to an overall PCE of 4.47% ( $V_{\text{OC}}$  791 mV,  $J_{\text{SC}}$  7.52  $\text{mA cm}^{-2}$  and FF 75.1%), outperforming in all photovoltaic parameters (except  $V_{\text{OC}}$ ) its liquid counterpart.

### 2.3. Design of Experiment (DoE) on the devices stability

Without underestimating this result, the main goal behind the development of a gelled electrolyte is to confer a longer lifetime to the device. Therefore, we monitored the photovoltaic performances of a-DSSCs for several days; indeed, the adoption of DoE allowed us to evaluate the effect of each parameter (and combinations of them) on cell stability. The variation percentages were calculated for each photovoltaic parameter and the results for all samples (after 48 h) are reported in **Table S1** and **Figure S3**. To understand the different performance losses, multivariate analyses were computed for each PV response. Unfortunately, in this case DoE models were affected by a moderate fitting error, which limited the speculation on possible interactions between factors. However, some main effects on stability are clearly detectable from **Figure S3**. As expected, the presence of XG (yellow bars in **Figure S3**) was the main factor influencing both  $J_{\text{SC}}$  and PCE stability. In liquid electrolytes, both of these parameters decreased by about 15%, while they were stable (when XG = 1.5 wt%) or even increased (when XG = 3 wt%) in gelled electrolytes. Thus, this improvement was directly dependent on the amount of XG added in the electrolyte formulation. A possible explanation of the ameliorated performances over time could be related to the improved permeation of the electrolyte into the

TiO<sub>2</sub> mesopores, which required a longer time in case of gelled matrix richer in XG. A better permeation should correspond to a more effective interaction at the TiO<sub>2</sub>-dye/electrolyte interface, leading to higher J<sub>SC</sub>. Interestingly, V<sub>OC</sub> and FF were quite stable over the aging period and their stabilities did not seem to be influenced by XG, but rather by redox shuttle component concentrations.

The stabilizing effect of XG was further confirmed by comparing the most stable cells, measured after 5 days from device sealing and reported in **Table 3**. Indeed, liquid and quasi-solid devices lost more than 20% and less than 5% of the initial PCE, respectively, Hence, XG matrix was proved to be able to entrap the solvent and to maintain the electrolyte properties and cell performances stable.

**Table 3.** Photovoltaic performance of the most stable a-DSSCs after 5 days of aging.

| Cell      | Co <sup>2+</sup><br>[M] | Co <sup>2+</sup> /Co <sup>3+</sup> | XG<br>[%wt] | V <sub>OC</sub><br>[mV] | J <sub>SC</sub><br>[mA cm <sup>-2</sup> ] | FF<br>[%] | PCE<br>[%] | ΔPCE<br>[%] |
|-----------|-------------------------|------------------------------------|-------------|-------------------------|---|-----------|------------|-------------|
| <b>5</b>  | 0.14                    | 4                                  | 0           | 821                     | 5.55                                      | 74.2      | 3.38       | -18.6       |
| <b>6</b>  |                         |                                    |             | 800                     | 6.35                                      | 60.6      | 3.08       | -24.3       |
| <b>7</b>  | 0.28                    | 4                                  | 0           | 768                     | 5.52                                      | 79.2      | 3.36       | -11.8       |
| <b>8</b>  |                         |                                    |             | 773                     | 5.49                                      | 80.6      | 3.42       | -16.2       |
| <b>12</b> | 0.14                    | 4                                  | 3           | 768                     | 7.51                                      | 49.6      | 2.86       | -5.0        |
| <b>16</b> |                         |                                    |             | 767                     | 7.15                                      | 70.4      | 3.86       | -2.5        |
| <b>17</b> | 0.21                    | 3                                  | 1.5         | 766                     | 7.76                                      | 69.5      | 4.13       | -7.6        |
| <b>18</b> |                         |                                    |             | 783                     | 6.52                                      | 73.5      | 3.75       | -1.1        |

### 3. Conclusion

Truly aqueous electrolytes based on cobalt complex mediators have been successfully prepared and gelled by the addition of XG. The amount of XG polymer, concentration of Co<sup>2+</sup> and its ratio with Co<sup>3+</sup> were thoroughly investigated by means of DoE. The gelation with XG matrix allowed increased photocurrent density values. Above all, the highest performances were achieved with 1.5 wt% XG, 0.21 M Co(bpy-pz)<sub>2</sub>Cl<sub>2</sub> and a Co<sup>2+</sup>/Co<sup>3+</sup> ratio equal to 3 (*i.e.*, 0.07 M Co(bpy-pz)<sub>2</sub>Cl<sub>3</sub>), leading to an overall PCE of 4.47% (V<sub>OC</sub> 791 mV, J<sub>SC</sub> 7.52 mA cm<sup>-2</sup> and FF 75.1%). This value is one of the highest ever reported in the literature for a gelled aqueous

electrolyte and the highest for a cobalt-based quasi-solid a-DSSC. Moreover, the efficiency of gelled cells was shown to be stable over the explored five days of aging.

Overall, this work demonstrates the feasibility of simple and low-cost gelled aqueous electrolytes based on cobalt complexes.

#### 4. Experimental Section/Methods

*Device assembly and testing:* The general procedures adopted to prepare each substrate and to assembly final devices have been already reported in previous papers of our group and are recalled hereafter. Transparent conductive oxide glasses based on fluorine-doped tin oxide (FTO) ( $15 \Omega \text{ sq}^{-1}$ ) were washed with water and detergent, then with ethanol and finally dried with compressed air. A nanometric compact layer (acting as a blocking layer) of  $\text{TiO}_2$  was deposited by spray-pyrolysis ( $400^\circ\text{C}$  for 1 h) from a titanium diisopropoxide bis(acetylacetonate) solution in ethanol. After cooling the substrate to room temperature, a layer of commercial  $\text{TiO}_2$  paste (18NR-T by Greatcell Solar Materials, average particle diameter up to 20 nm) was manually screen-printed on the so-obtained substrates and sintered at  $520^\circ\text{C}$  for 30 min (ramp:  $10^\circ\text{C min}^{-1}$ ). The sintering temperature was chosen according to technical datasheets. The final thickness of mesoporous  $\text{TiO}_2$  electrode was  $4 \mu\text{m}$ . It was then post-treated by dipping into a  $\text{TiCl}_4$  aqueous solution (40 mM,  $70^\circ\text{C}$ , 30 min) and subsequently washed with de-ionized water and ethanol. Before the sensitization procedure, the electrode was heated at  $450^\circ\text{C}$  for 30 min and then immersed, still hot, in the sensitization solution (*vide infra*). The sensitization was performed in a tilting multi-reactor (Syncore Polyvap Büchi, Labortechnik AG), that allowed control of the stirring rate as well as the temperature. Sensitization process sensibly depends on the nature of the employed dyes. The photoanodes were dipped in a MK2 (0.3 mM) solution in acetonitrile/*t*-butanol/toluene (1:1:1), also containing CDCA as disaggregating agent (9 mM). After dye sensitization, the electrodes were rinsed with acetone to eliminate the non-chemisorbed dye molecules. Platinum counter-electrodes were made by

spreading a 5 mM  $\text{H}_2\text{PtCl}_6$  solution in ethanol onto a FTO glass, followed by heating step at 400 °C for 30 min. To prepare the electrolytes, MilliQ water ( $18\ \Omega\ \text{cm}^{-1}$  at 25 °C) was obtained with a Direct-Q 3UV Water Purification System by Millipore. Water was saturated with CDCA: an excess of CDCA was suspended in water and stirred at 40 °C overnight. Then, after cooling the solution at room temperature, the excess of CDCA was filtered using filter paper. For liquid electrolytes, the cobalt-based redox couple and 0.4 M NMBI were added to the CDCA solution with stirring and gentle heating. For jellified electrolytes, the proper amount of XG (1.5 or 3.0 wt% by weight) was simply added and dissolved into the liquid electrolyte.

The final assembly procedure depends on the physical state of the electrolyte used. For liquid electrolytes, a gasket of polymeric thermoplastic film (Surlyn, DuPont) was placed between photoanode and counter electrode and heated up to 110 °C for 30 s in a hot press. Then, the cell was filled with the electrolyte through a hole by vacuum technique and finally sealed with glue. For gelled solutions with high viscosity, the electrolyte (2 mg) was spread on the sensitized  $\text{TiO}_2$  electrode with a spatula, then the cell was sealed in a hot press as described above.

Devices were tested under 1 sun irradiation (AM 1.5G) by means of a 3A class sun simulator equipped with a 450 W xenon light source (SOL3A, Newport Corp., CA, USA) and a sunlight filter (Schott K113 Tempax, Präzisions Glas & Optik GmbH, Germany), connected to a digital source meter (2400, Keithley Instrument Inc., OH, USA).

### Supporting Information

Supporting Information is available from the Wiley Online Library.

### Acknowledgements

((Acknowledgements, general annotations, funding. Other references to the title/authors can also appear here, such as “Author 1 and Author 2 contributed equally to this work.”))

Received: ((will be filled in by the editorial staff))

Revised: ((will be filled in by the editorial staff))

Published online: ((will be filled in by the editorial staff))

### References

- [1] M. Grätzel, *J. Photochem. Photobiol. C Photochem. Rev.* **2003**, *4*, 145–153.
- [2] M. Bonomo, A. Di Carlo, D. Dini, *J. Electrochem. Soc.* **2018**, *165*, H889–H896.
- [3] J. Gong, K. Sumathy, Q. Qiao, Z. Zhou, *Review on Dye-Sensitized Solar Cells (DSSCs): Advanced Techniques and Research Trends*, **2017**.
- [4] W. Yang, M. Söderberg, A. I. K. Eriksson, G. Boschloo, *RSC Adv.* **2015**, *5*, 26706–26709.
- [5] N. Mariotti, M. Bonomo, L. Fagiolari, N. Barbero, C. Gerbaldi, F. Bella, C. Barolo, *Green Chem.* **2020**, Accepted Manuscript.
- [6] J. Wu, Z. Lan, J. Lin, M. Huang, Y. Huang, L. Fan, G. Luo, *Chem. Rev.* **2015**, *115*, 2136–2173.
- [7] H. Iftikhar, G. G. Sonai, S. G. Hashmi, A. F. Nogueira, P. D. Lund, *Materials (Basel)*. **2019**, *12*, 1998.
- [8] L. Giribabu, R. Bolligarla, M. Panigrahi, *Chem. Rec.* **2015**, *15*, 760–788.
- [9] S. A. Sapp, C. M. Elliott, C. Contado, S. Caramori, C. A. Bignozzi, *J. Am. Chem. Soc.* **2002**, *124*, 11215–11222.
- [10] H. N. Tsao, C. Yi, T. Moehl, J. H. Yum, S. M. Zakeeruddin, M. K. Nazeeruddin, M. Grätzel, *ChemSusChem* **2011**, *4*, 591–594.
- [11] S. M. Feldt, E. A. Gibson, E. Gabrielsson, L. Sun, G. Boschloo, A. Hagfeldt, *J. Am. Chem. Soc.* **2010**, *132*, 16714–16724.
- [12] K. Kakiage, Y. Aoyama, T. Yano, K. Oya, J. I. Fujisawa, M. Hanaya, **2015**, *51*, 15894–15897.
- [13] M. H. Khanmirzaei, S. Ramesh, K. Ramesh, *Ionics (Kiel)*. **2015**, *21*, 2383–2391.
- [14] S. Zhang, G.-Y. Y. Dong, B. Lin, J. Qu, N.-Y. Y. Yuan, J.-N. N. Ding, Z. Gu, *Sol. Energy* **2016**, *127*, 19–27.
- [15] Y. Fang, J. Zhang, X. Zhou, Y. Lin, S. Fang, *Electrochem. commun.* **2012**, *16*, 10–13.
- [16] H.-F. Lee, J.-J. Kai, P.-C. Liu, W.-C. Chang, F.-Y. Ouyang, H.-T. Chan, *J.*

- Electroanal. Chem.* **2012**, *687*, 45–50.
- [17] X. Wang, S. a Kulkarni, B. I. Ito, S. K. Batabyal, K. Nonomura, C. C. Wong, M. Grätzel, S. G. Mhaisalkar, S. Uchida, *ACS Appl. Mater. Interfaces* **2013**, *5*, 444–450.
- [18] B. Li, L. Wang, B. Kang, P. Wang, Y. Qiu, *Sol. Energy Mater. Sol. Cells* **2006**, *90*, 549–573.
- [19] W. Xiang, W. Huang, U. Bach, L. Spiccia, *Chem. Commun.* **2013**, *49*, DOI 10.1039/c3cc44555k.
- [20] M. Bhagavathi Achari, V. Elumalai, N. Vlachopoulos, M. Safdari, J. Gao, J. M. Gardner, L. Kloo, *Phys. Chem. Chem. Phys.* **2013**, *15*, 17419–17425.
- [21] F. Bella, N. Vlachopoulos, K. Nonomura, S. M. Zakeeruddin, M. Grätzel, C. Gerbaldi, A. Hagfeldt, *Chem. Commun.* **2015**, *51*, 16308–16311.
- [22] F. Bella, A. Sacco, G. Massaglia, A. Chiodoni, C. F. Pirri, M. Quaglio, *Nanoscale* **2015**, *7*, 12010–12017.
- [23] Y. Wang, *Sol. Energy Mater. Sol. Cells* **2009**, *93*, 1167–1175.
- [24] S. Rudhzhiah, A. Ahmad, I. Ahmad, N. S. Mohamed, *Electrochim. Acta* **2015**, *175*, 162–168.
- [25] T. Daeneke, Y. Uemura, N. W. Duffy, A. J. Mozer, N. Koumura, U. Bach, L. Spiccia, *Adv. Mater.* **2012**, *24*, 1222–1225.
- [26] A. Glinka, M. Gierszewski, M. Ziótek, *J. Phys. Chem. C* **2018**, *122*, 8147–8158.
- [27] R. K. R. K. Kokal, S. Bhattacharya, L. S. L. S. Cardoso, P. B. P. B. Miranda, V. R. V. R. Soma, P. Chetti, D. Melepurath, S. S. K. S. S. K. Raavi, *Sol. Energy* **2019**, *188*, 913–923.
- [28] H. Ellis, R. Jiang, S. Ye, A. Hagfeldt, G. Boschloo, *Phys. Chem. Chem. Phys.* **2016**, *18*, 8419–8427.
- [29] F. Bella, L. Porcarelli, D. Mantione, C. Gerbaldi, C. Barolo, M. Grätzel, D. Mecerreyes, *Chem. Sci.* **2020**, *11*, 1485–1493.

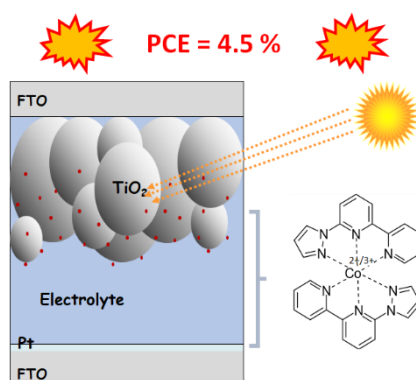


- [30] W. Xiang, D. Chen, R. A. Caruso, Y.-B. Cheng, U. Bach, L. Spiccia, *ChemSusChem* **2015**, 8, 3704–3711.
- [31] W. Xiang, D. Chen, R. A. Caruso, Y. B. Cheng, U. Bach, L. Spiccia, *ChemSusChem* **2015**, 8, 3704–3711.
- [32] F. García-Ochoa, V. . Santos, J. . Casas, E. Gómez, *Biotechnol. Adv.* **2000**, 18, 549–579.
- [33] S. Galliano, F. Bella, M. Bonomo, G. Viscardi, C. Gerbaldi, G. Boschloo, C. Barolo, *Nanomaterials* **2020**, 10, 1585.
- [34] J. G. Krishna, P. K. Ojha, S. Kar, K. Roy, J. Leszczynski, *Nano Energy* **2020**, 70, 104537.
- [35] R. Singh, A. R. Polu, B. Bhattacharya, H. W. Rhee, C. Varlikli, P. K. Singh, *Renew. Sustain. Energy Rev.* **2016**, 65, 1098–1117.
- [36] Modde 11 Software; Umetrics: Umeå, Sweden, 2015; Available online: <https://umetrics.com/kb/modde-11> (accessed on 22 November 2020).

Design of Experiment is successfully applied to engineer the composition of the electrolyte in quasi-solid aqueous DSSCs employing a cobalt-based complex as redox mediator and Xanthan Gum as jellifying agent. The optimized composition leads to photoconversion efficiency approaching 5% and remarkable stability, losing less than 2% of initial efficiency after 5 days of accelerated aging.

*S. Galliano, F. Bella\*, M. Bonomo\*, F. Giordano, M. Grätzel, G. Viscardi, A. Hagfeldt, C. Gerbaldi, C. Barolo*

### **Xanthan-based hydrogel for stable and efficient quasi-solid truly aqueous DSSC with cobalt mediator**



## Supporting Information

### Xanthan-based hydrogel for stable and efficient quasi-solid truly aqueous DSSC with cobalt mediator

*Simone Galliano, Federico Bella\*, Matteo Bonomo\*, Fabrizio Giordano, Michael Grätzel, Guido Viscardi, Anders Hagfeldt, Claudio Gerbaldi, Claudia Barolo*

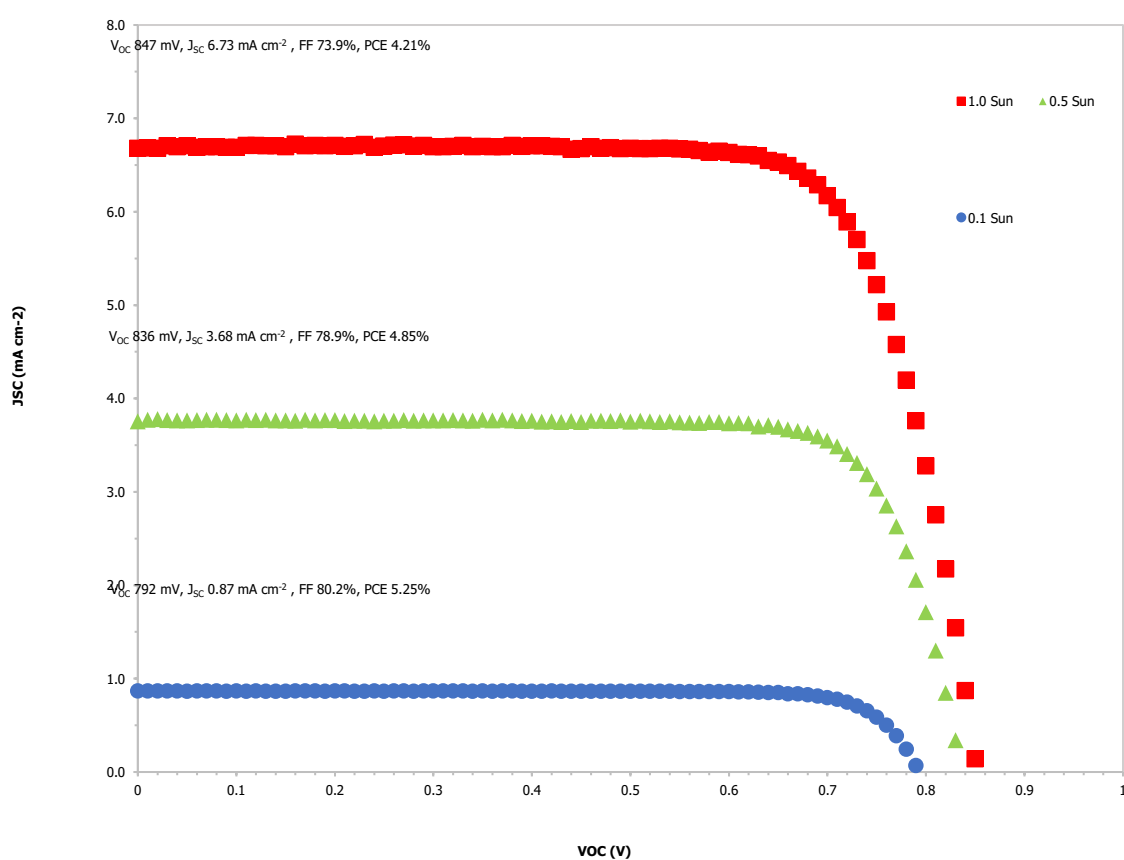


**Figure S1.** J-V curve (with PV parameters) under different light intensities of cell filled with  $\text{Co}(\text{bpy-pz})_2\text{Cl}_2$  0.13 M,  $\text{Co}(\text{bpy-pz})_2\text{Cl}_3$  0.04 M and NMBI 0.4 M in CDCA-saturated water.

**Table S1.** Performance variation of photovoltaic parameters for a-DSSCs after  $\approx 48$  h from device sealing (some cells are not reported due to device failure).

| Cell      | Co <sup>2+</sup><br>[M] | Co <sup>2+</sup> /Co <sup>3+</sup> | XG<br>[wt%] | $\Delta V_{oc}$<br>[%] | $\Delta J_{sc}$<br>[%] | $\Delta FF$<br>[%] | $\Delta PCE$<br>[%] |
|-----------|-------------------------|------------------------------------|-------------|------------------------|------------------------|--------------------|---------------------|
| <b>1</b>  | 0.14                    | 2                                  | 0           | −0.2                   | −14.5                  | 1.1                | −13.8               |
| <b>2</b>  |                         |                                    |             | −0.8                   | −21.1                  | −1.0               | −22.8               |
| <b>3</b>  | 0.28                    | 2                                  | 0           | −1.0                   | −6.0                   | −0.8               | −7.6                |
| <b>4</b>  |                         |                                    |             | −1.5                   | −10.4                  | −1.8               | −13.3               |
| <b>5</b>  | 0.14                    | 4                                  | 0           | −1.4                   | −11.5                  | −0.5               | −13.3               |
| <b>6</b>  |                         |                                    |             | −1.0                   | −6.6                   | −15.2              | −21.6               |
| <b>7</b>  | 0.28                    | 4                                  | 0           | −2.9                   | −6.9                   | −1.6               | −8.9                |
| <b>8</b>  |                         |                                    |             | −1.3                   | −12.3                  | −0.1               | −13.5               |
| <b>9</b>  | 0.14                    | 2                                  | 3           | −1.7                   | 1.6                    | −1.3               | −1.5                |
| <b>10</b> | 0.28                    | 2                                  | 3           | −1.4                   | 1.0                    | 0.4                | 0.0                 |
| <b>11</b> |                         |                                    |             | −1.3                   | 1.6                    | −1.2               | −0.9                |
| <b>12</b> | 0.14                    | 4                                  | 3           | −0.1                   | 5.4                    | −5.3               | −0.3                |
| <b>14</b> | 0.28                    | 4                                  | 3           | −1.3                   | 5.6                    | −3.5               | 0.6                 |
| <b>16</b> | 0.21                    | 3                                  | 1.5         | −1.1                   | −2.1                   | −0.8               | −4.0                |
| <b>17</b> |                         |                                    |             | −1.4                   | 1.8                    | −1.5               | −1.1                |
| <b>18</b> |                         |                                    |             | −1.3                   | 0                      | −2.2               | −3.4                |

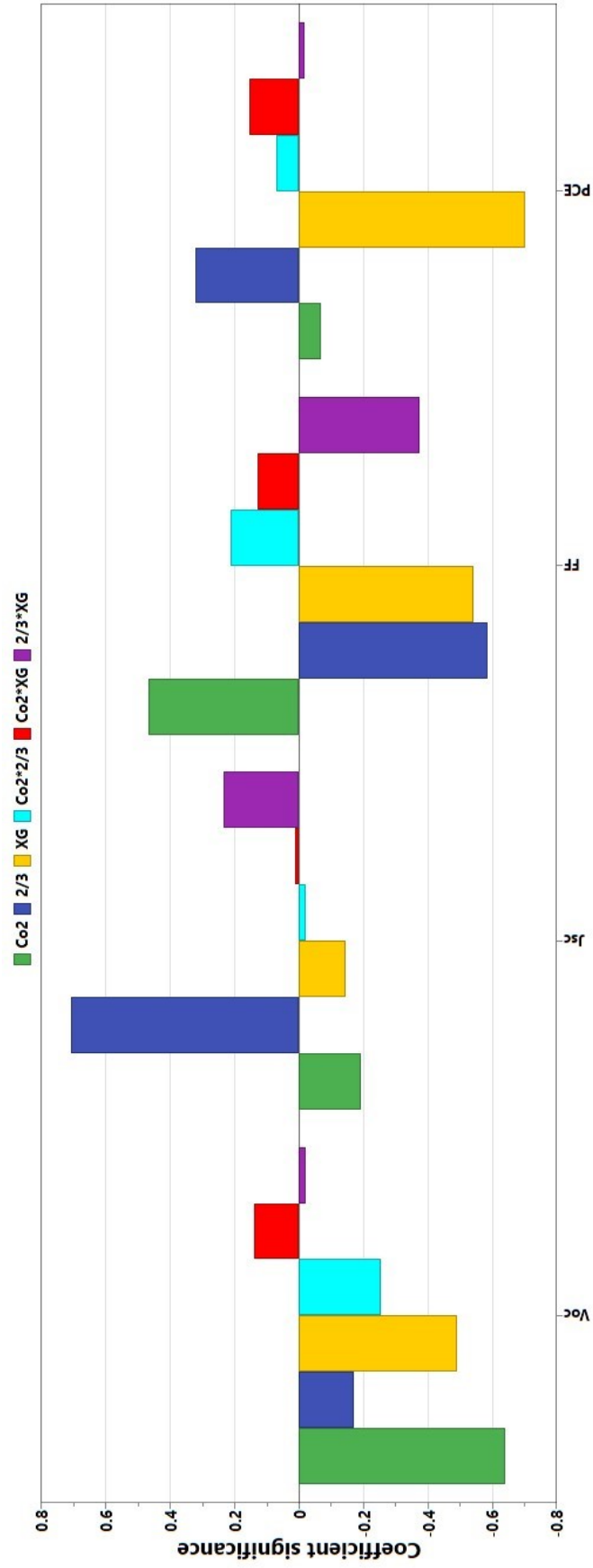


**Figure S2.** Coefficient significances of each model term on selected responses.

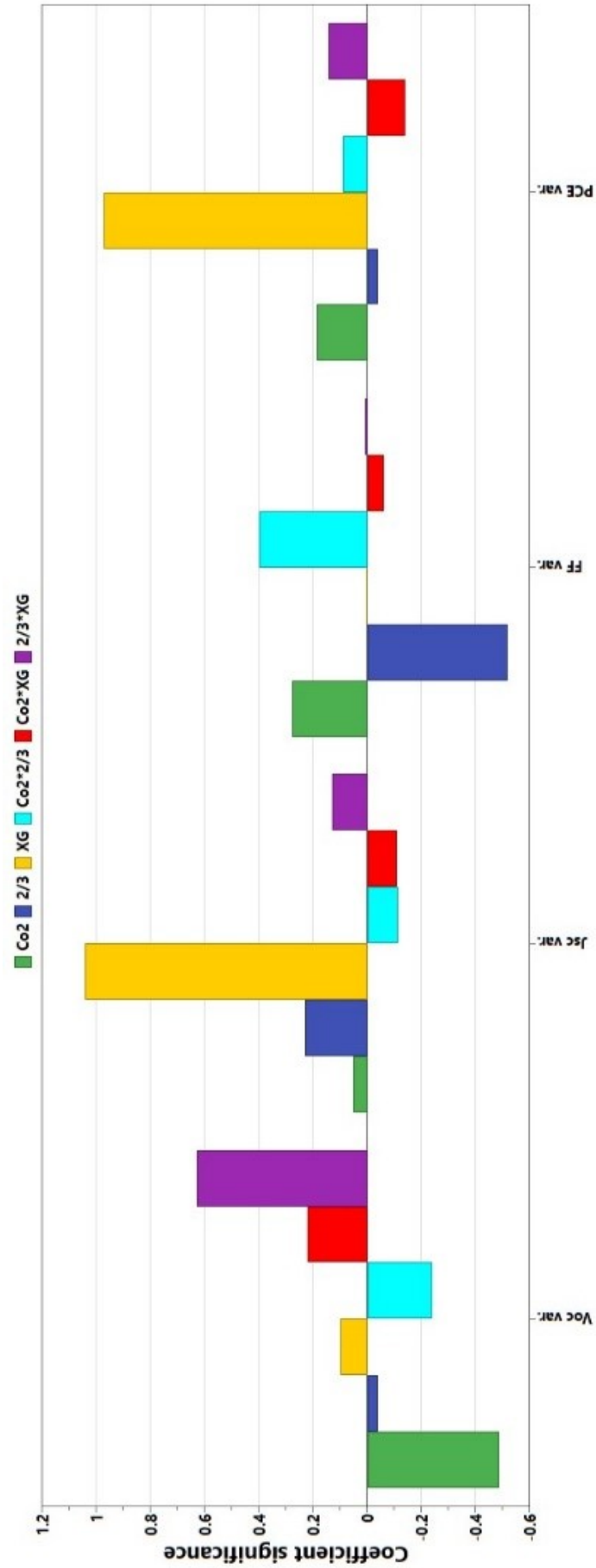


**Figure S3.** Coefficient significances of each model term related to the PV performance variations.